

Adaptive Off-Time Control for Variable-Frequency, Soft-Switched Flyback Converter at Light Loads

Yuri Panov and Milan M. Jovanović, *Fellow, IEEE*

Abstract—The soft switching of a flyback converter can be achieved by operating the circuit in the critical conduction mode. However, the critical-mode operation at light loads cannot be maintained due to a very high switching frequency and the loss of the output voltage regulation. A control which regulates the output down to the zero load and maintains soft switching at light loads is proposed. The proposed control scheme was implemented in the 380-V/19-V, 65-W flyback dc/dc converter.

Index Terms—Adaptive control, flyback converter, soft switching, variable frequency.

I. INTRODUCTION

DUE to the minimum number of semiconductor and magnetic components, a flyback converter is a very attractive candidate for off-line low-cost power supplies which require input/output isolation. Since the voltage on the primary switch at the turn-on instant is high and the associated capacitive turn-on loss is substantial, the switch soft turn-on is highly desirable. The soft switching is also helpful in reducing the size and loss of the EMI filter. The soft turn-on of the primary switch is accomplished in the flyback converter operating in the critical conduction mode, i.e., at the boundary of continuous and discontinuous conduction modes (CCM/DCM). The critical mode of operation requires a variable frequency (VF) control to regulate the output voltage against input-voltage and load variations. Operation of the VF flyback converter in the critical mode is discussed in [1]–[6]. However, the VF critical-mode control suffers from a wide frequency range and loss of the output voltage regulation at light load. Namely, for this control, the switch on-time should decrease, as the load current decreases. However, since the minimum on-time of the controller is limited by its internal delays, the converter operating in the critical mode cannot maintain the output regulation at light load.

This problem can be alleviated by limiting the minimum controller off-time to a fixed value, so that converter switches from the critical operation mode at high load to the DCM with a constant off-time at light loads, as implemented in [3], [4]. However, it was found experimentally that the constant off-time control could not maintain the output regulation as the load current approaches zero value. The control implementations in [3], [4] also do not provide soft switching at light loads.

The objective of the paper is to propose a simple VF converter control which maintains the output regulation and soft switching in the entire load range.

Manuscript received September 3, 1999; revised March 15, 2002. Recommended by Associate Editor M. E. Elbuluk.

The authors are with the Delta Products Corporation, Power Electronics Laboratory, Research Triangle Park, NC 27709 USA.

Publisher Item Identifier 10.1109/TPEL.2002.800958.

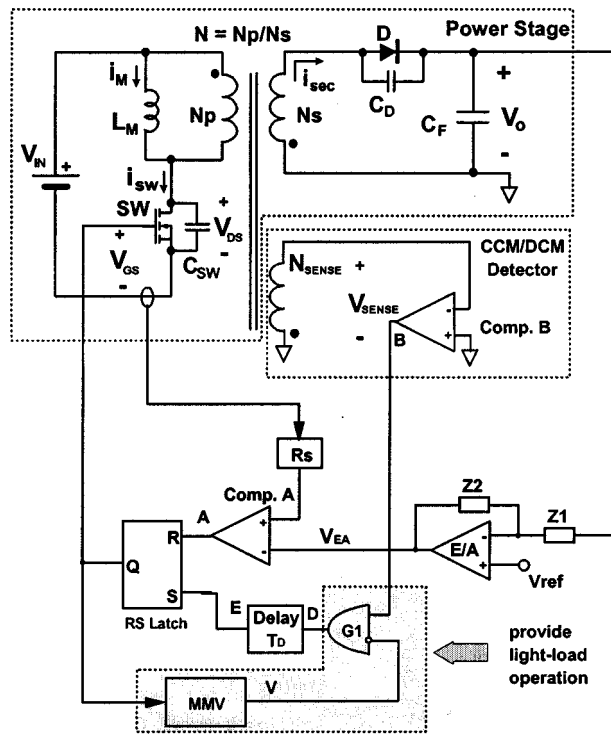
II. CONVENTIONAL OFF-TIME CONTROL OF VF FLYBACK CONVERTER AT LIGHT LOADS

A. Principle of Operation

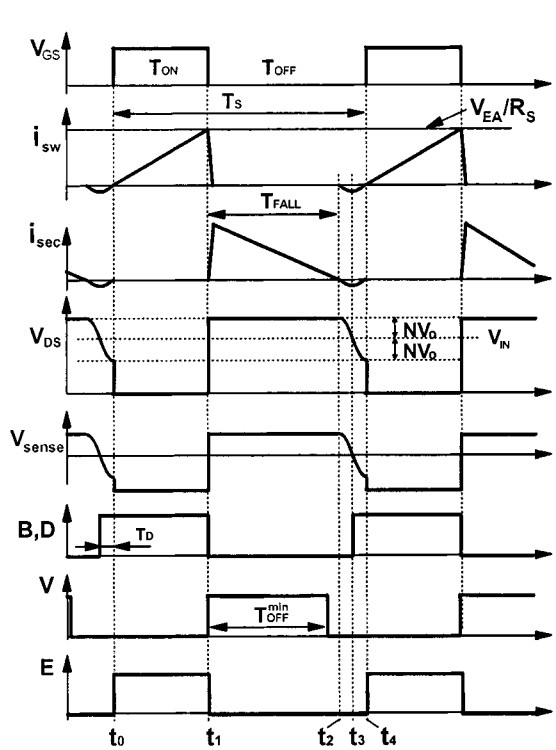
The functional diagram of the VF flyback converter with a constant off-time control at light loads and its key waveforms are shown in Fig. 1. The switching cycle starts at the instant $t = t_0$, when switch SW turns on. During the interval $[t_0, t_1]$, switch current i_{SW} increases linearly. Output signal V_{EA} of error amplifier EA is compared with the sensed switch current $i_{SW} \cdot R_S$. When the switch current reaches the V_{EA}/R_S level at $t = t_1$, the RS latch, which controls the gate drive, is reset. After switch SW is turned off, transformer magnetizing current i_M commutates from the primary winding to the secondary one and linearly decreases during the interval $[t_1, t_2]$. When secondary current i_{SEC} reaches zero at the instant $t = t_2$, transformer magnetizing inductance L_M starts resonating with parasitic capacitances of the primary switch C_{SW} and secondary rectifier C_D . The zero crossing of the secondary current is sensed indirectly by the CCM/DCM detector, which monitors voltage V_{SENSE} across sensing winding N_{SENSE} . Voltage V_{SENSE} resonates, as shown in Fig. 1(b). When voltage V_{SENSE} goes negative at $t = t_3$, detector output signal **B** becomes high. The way the RS latch is set depends on the load. At heavy loads [see Fig. 1(b)], secondary current fall time T_{FALL} is longer than the duration of the output pulse V of the monostable multivibrator (MMV). Then, at $t = t_3$ detector output signal **B** propagates through gate G1, and after delay T_D sets the latch at the instant $t = t_4$. Delay T_D between V_{SENSE} zero-crossing and the RS latch set is selected to be a quarter of the resonant period and provides turn-on of switch SW with the voltage $V_{IN} - N \cdot V_O$ across it. As a result, the switching loss is substantially reduced. At light loads [see Fig. 1(c)], the secondary current fall time is shorter than the MMV output pulse duration. Then, the output signal of the CCM/DCM detector cannot propagate through gate G1 until the MMV output pulse expires at the instant $t = t_4$. Therefore, at light load, the switch off-time is determined by the MMV output pulse duration.

B. Limitations

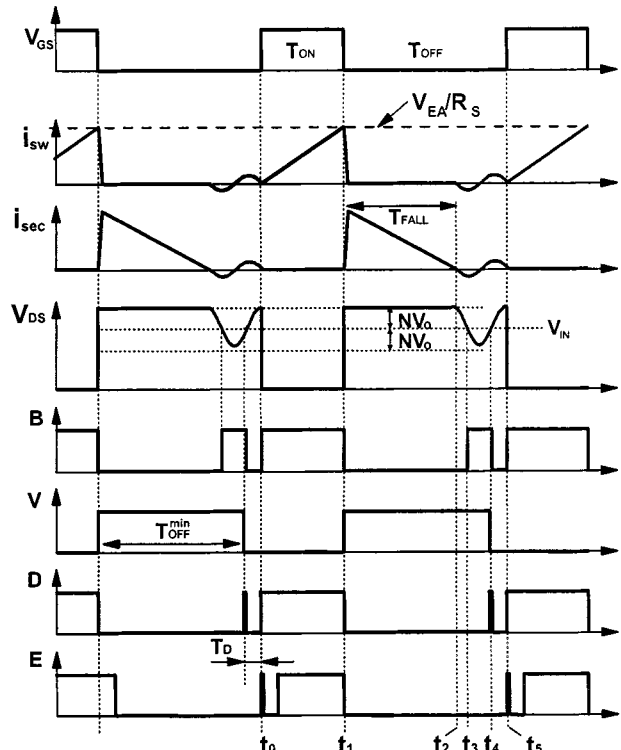
The analysis in this Section facilitates the explanation of limitations of the constant off-time control at light loads. All converter components were assumed ideal for analysis purposes. The analysis was performed for the 380-V/19-V, 65-W flyback converter. The full-load switching frequency of the converter was selected to be 35 kHz which is above the audible range. The corresponding transformer magnetizing inductance was $L_M =$



(a)



(b)



(c)

Fig. 1. Conventional control of VF flyback converter: (a) functional diagram, (b) heavy-load waveforms, and (c) light-load waveforms.

1.27 mH. To keep the switch voltage stress below 600 V, the transformer has turns ratio $N = 5 : 1$.

The peak value I_{PEAK} of switch current i_{sw} is related to on-time T_{ON} and fall time of the secondary current T_{FALL} as

$$I_{PEAK} = \frac{V_{IN} \cdot T_{ON}}{L_M} \quad (1)$$

$$I_{PEAK} = \frac{V_O \cdot T_{FALL}}{L_M} \cdot N. \quad (2)$$

Load current is equal to the average value of the secondary current

$$I_O = \frac{I_{PEAK} \cdot T_{FALL}}{2 \cdot T_S} \cdot N. \quad (3)$$

From (1) and (2), the relationship between the on-time and fall time is

$$\frac{T_{ON}}{T_{FALL}} = M \cdot N \quad (4)$$

where $M = V_O/V_{IN}$ is the voltage conversion ratio. From (2) and (3), one can derive

$$I_O = \frac{V_O \cdot (N \cdot T_{FALL})^2}{2 \cdot L_M \cdot T_S}. \quad (5)$$

In the critical mode

$$T_S = T_{ON} + T_{FALL}. \quad (6)$$

Combining (4)–(6) produces

$$T_{FALL} = \frac{I_O}{V_O} \cdot \frac{2 \cdot L_M}{N^2} \cdot (1 + M \cdot N) \quad (7)$$

$$T_S = \frac{I_O}{V_O} \cdot \frac{2 \cdot L_M}{N^2} \cdot (1 + M \cdot N)^2. \quad (8)$$

The latter equation indicates that in the critical mode the switching frequency is inversely proportional to the load current. Theoretically, the switching frequency approaches infinity as the load current approaches zero. This implies that in the critical mode the converter would suffer from an extremely wide frequency range and excessive switching losses at light loads.

Another limitation of the critical mode operation at light loads comes from the fact that, practically, the minimum on-time of the controller is limited to 0.5–0.9 μs by the delays of the comparator and logic circuitry of the controller IC. If the required on-time becomes smaller than the control IC minimum on-time, the controller can no longer maintain the output regulation. Reduction of the controller minimum on-time time is possible by refining the IC circuitry, but it causes a sensitive increase of the IC cost.

From (4) and (7), the minimum output power value P_{Ocrit}^{\min} at which the controller is able to regulate the output in the critical mode is equal

$$P_{Ocrit}^{\min} = \frac{T_{ON}^{\min} \cdot V_{IN} \cdot V_O \cdot N}{L_M \cdot (1 + M \cdot N)}. \quad (9)$$

For $T_{ON}^{\min} = 0.8 \mu\text{s}$, P_{Ocrit}^{\min} value computed from (9) is 8.6 W. The switching frequency which corresponds to P_{Ocrit}^{\min} is close to 250 kHz. For lower loads, the output-voltage regulation of the VF converter in the critical mode cannot be maintained.

The output regulation at the loads below P_{Ocrit}^{\min} can be achieved by operating the converter in DCM with the constant off-time T_{OFF}^{\min} . For the constant off-time control, $T_S = T_{ON} + T_{OFF}^{\min}$, and expressions (4), (5) are employed to derive the minimum output power at which the controller is still able to regulate the output

$$P_{Odc}^{\min} = \frac{V_{IN}^2 \cdot T_{ON}^{\min 2}}{2 \cdot L_M \cdot (T_{ON}^{\min} + T_{OFF}^{\min})}. \quad (10)$$

To facilitate explanation of the constant off-time control limitation, the minimum output power attainable in the critical mode and in DCM is graphed in Fig. 2 as a function of the minimum

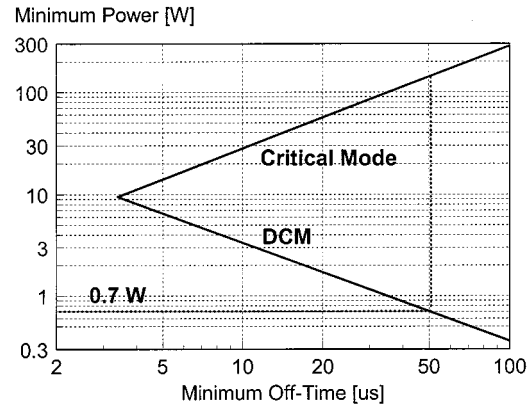


Fig. 2. Calculated minimum load attainable in critical conduction mode and in DCM for conventional off-time control.

off-time. The minimum output power attainable with the constant off-time control was computed based on (10), whereas the minimum output power attainable with the critical-mode control was computed based on (4) and (9). If the converter is expected to operate down to 0.7 W load, then, based on Fig. 2, the minimum off-time should be chosen to be 51 μs . However, for $T_{OFF}^{\min} = 51 \mu\text{s}$, the critical-mode operation starts only at the load above 100 W. This means that the 65-W converter will operate in DCM in the entire load range. As the T_{OFF}^{\min} value increases, the output regulation range increases, but at the same time the load level at which converter shifts from the critical mode to the DCM increases. The trade-off between the output regulation at light load and critical mode of operation at high load cannot be satisfied for the conventional off-time control.

Also, as can be seen from Fig. 1(c), the conventional control does not provide turn-on of the switch with the minimum voltage across it. Therefore, the conventional control loses soft switching at light loads.

III. PROPOSED OFF-TIME CONTROL OF VF FLYBACK CONVERTER AT LIGHT LOAD

A. Principle of Operation

The functional diagram of the proposed control is shown in Fig. 3(a). Heavy-load waveforms of the proposed control coincide with those of the conventional control, shown in Fig. 1(b). The key waveforms of the proposed control at light loads are shown in Fig. 3(b). Different from the conventional control, the proposed controller contains the D flip-flop between the output of gate G1 and the input of the delay block. The control circuit operates as follows. MMV output pulse V ends at the instant $t = t_4$. However, the flip-flop output stays low until voltage V_{SENSE} changes its polarity from positive to negative at $t = t_5$. At the same instant, output signal B of the CCM/DCM detector changes from “0” to “1.” As the result, after delay T_D , the RS latch is set and switch SW turns ON at the instant $t = t_6$.

To solve the problem of the output regulation at light loads, the proposed control adaptively increases the off-time as the load decreases. To implement the adaptive control, the MMV pulse duration is adjusted in accordance with error amplifier output signal V_{EA} which indirectly carries information about the load. The MMV implementation is shown in Fig. 4. The

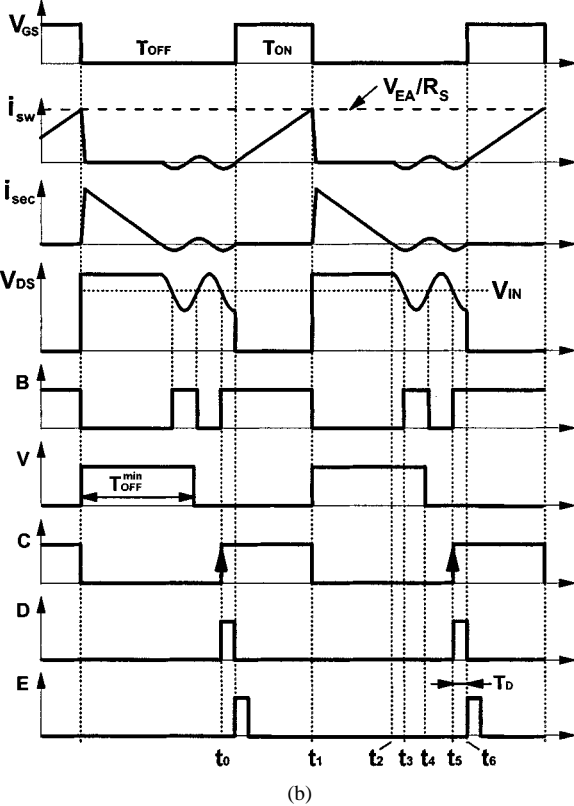
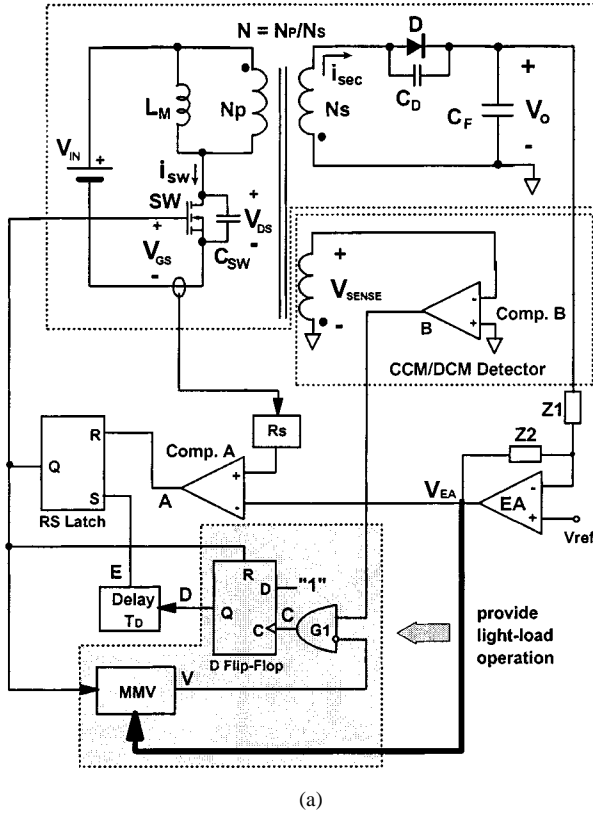


Fig. 3. Proposed VF flyback converter control: (a) functional diagram and (b) light-load waveforms.

duration of MMV output pulse V is adjusted by varying the comparator threshold as a function of the error amplifier output signal V_{EA} . In Fig. 4(a), capacitor C is charged through the

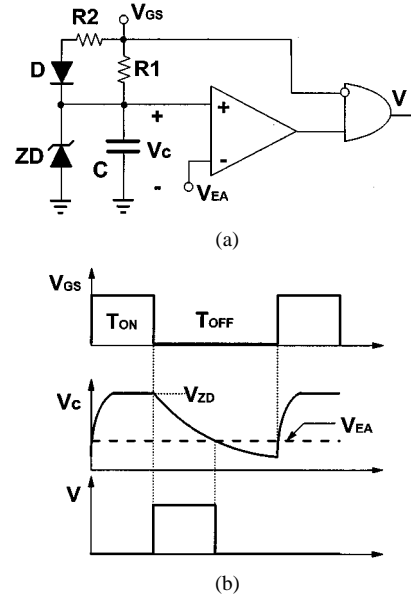


Fig. 4. Implementation of monostable multivibrator with a variable pulse width: (a) functional diagram and (b) key waveforms.

parallel combination of resistors $R1$ and $R2$ during on-time of the switch T_{ON} , and is discharged through resistor $R1$ during off-time T_{OFF} . Time constant $\tau_1 = R1 \cdot C$ is selected to be comparable with the maximum T_{OFF} value, while time constant $\tau_2 = (R1||R2) \cdot C$ is selected small enough to guarantee charge of capacitor C to Zener diode breakdown voltage V_{ZD} during minimum T_{ON} . Zener diode ZD assures charging of capacitor C to the same level independently of the magnitude of the gate-drive signal.

The relationship between the off-time and signal V_{EA} on the inverting input of the MMV comparator is

$$V_{EA} = V_{ZD} \cdot \exp\left(-\frac{T_{OFF}^{min}}{\tau_1}\right). \quad (11)$$

At the switch turn-off instant

$$V_{EA} = I_{PEAK} \cdot R_S. \quad (12)$$

The solution of (1), (9), (11), and (12) produces the dependence of the off-time upon the output power in DCM which is plotted in Fig. 5. Fig. 5 also contains a plot of the on-time versus the load. The computed curves consist of two different pieces. For loads above 1.5 W, the on-time stays above its minimum value T_{ON}^{min} , and both T_{ON} and T_{OFF} change in response to the load variation. For loads below 1.5 W, the on-time has reached its minimum value, and only the off-time varies with load change. The relationship between the off-time in the critical mode and the load current is also plotted in Fig. 5. The intersection of the T_{OFF} curves corresponding to the critical mode and DCM shows the point where the converter changes its mode of operation. The change of the operation mode occurs at the 38-W load power.

B. Soft Switching at Light Load

To retain soft switching at light load, the proposed control turns on the switch when its drain-source voltage V_{DS} reaches

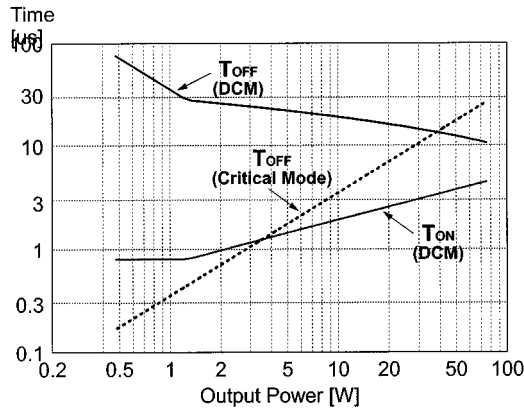


Fig. 5. Calculated on-time and off-time for the proposed control.

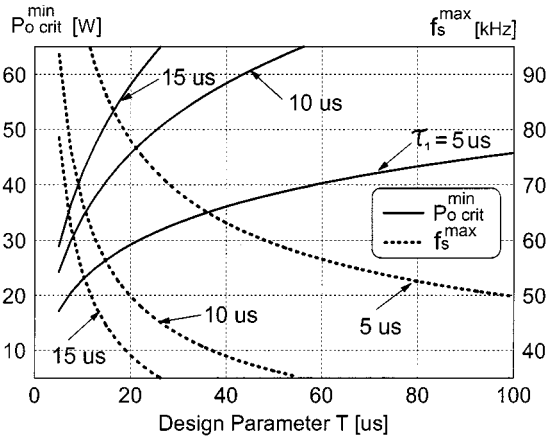


Fig. 6. Calculated dependence of minimum critical-mode load power and maximum switching frequency on control parameters.

the resonance valley. As shown in Fig. 3(a), the voltage V_{DS} minimum is detected by sensing the instant when voltage V_{SENSE} changes its polarity from positive to negative, and, then, delaying the switch turn-on instant for a quarter of the resonant period. After the MMV output pulse V has expired, the D flip-flop waits for the CCM/DCM detector output signal to transition from “0” to “1.” As soon as this event happens, the D flip-flop changes its output state from “0” to “1,” and after delay T_D turns on the switch. With delay T_D taken into account, the primary switch turn-on occurs exactly in the resonance valley of its drain-source voltage waveform.

C. Design Considerations

The control circuitry determines the output power P_{Ocrit}^{min} at which the converter shifts from the critical operation mode to the DCM. The P_{Ocrit}^{min} level is usually selected based on considerations of the circuit efficiency and frequency range. As the P_{Ocrit}^{min} value decreases, the operating frequency range increases. The desirable P_{Ocrit}^{min} value can be achieved by proper selection of Zener diode breakdown voltage V_{ZD} and time constant $\tau_1 = R_1 \cdot C$ of capacitor C in Fig. 4.

The calculated relationship between P_{Ocrit}^{min} , maximum operating frequency and design parameter $T = (L_M/V_{IN}) \cdot (V_{ZD}/R_S)$ for different τ_1 values is plotted in Fig. 6. As voltage V_{ZD} increases, the P_{Ocrit}^{min} level increases, and the maximum switching frequency decreases. The value of

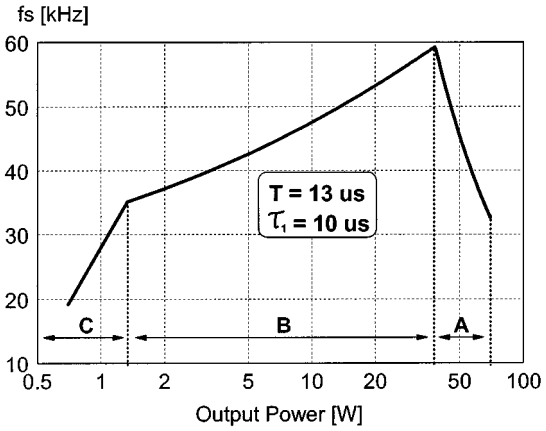


Fig. 7. Calculated switching frequency as a function of load for proposed control.

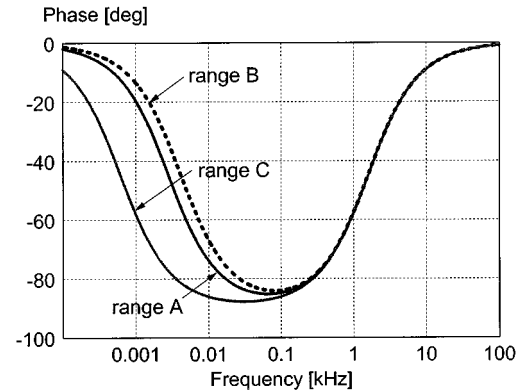
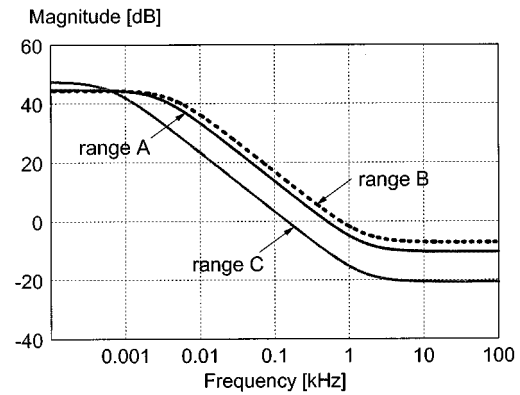


Fig. 8. Calculated frequency response of the control-to-output transfer function.

τ_1 is limited by several factors. A lower τ_1 value can result in a nearly zero voltage across capacitor C at the end of the off-time, causing the MMV comparator to become more susceptible to noise. A higher τ_1 value can result in an undesirably high P_{Ocrit}^{min} level, as can be seen from Fig. 6. These considerations determine the design range for the constant τ_1 .

The calculated dependence of the switching frequency upon load is plotted in Fig. 7 for selected design parameters. In the load range A (38–65 W), the converter operates in the critical mode, and the switching frequency increases from 35 to 58 kHz as the output power decreases. In the load range B (1.5–38 W), the converter operates in the DCM with variable on and off times. The frequency starts decreasing and drops to 35 kHz at

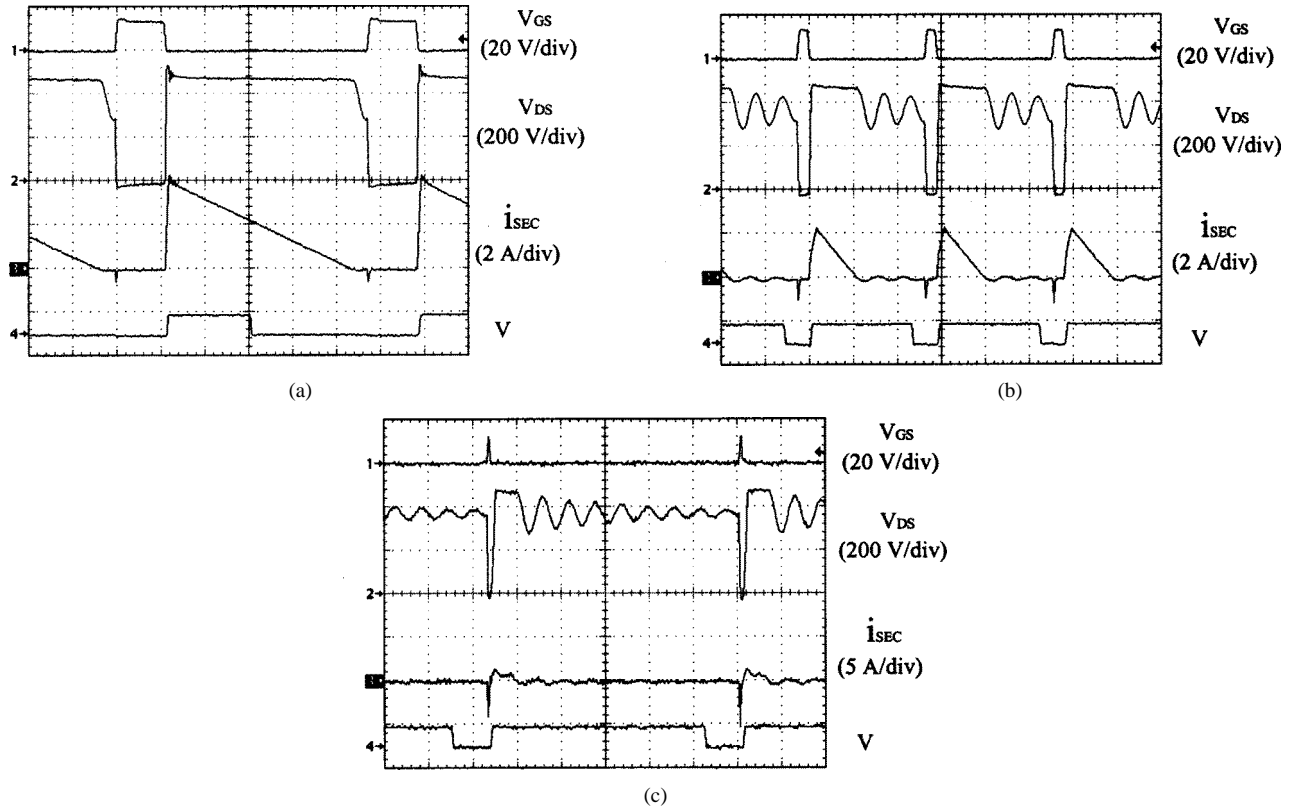


Fig. 9. Experimental waveforms of VF flyback converter at different loads: (a) $P_o = 70$ W, (b) $P_o = 10$ W, and (c) $P_o = 0.4$ W.

the 1.5 W load. At this power level, the on-time reaches its minimum value ($0.8 \mu\text{s}$). If the load is reduced below 1.5 W, the converter operates in the range C with the constant on-time, and the off-time grows rapidly as the load decreases. At the minimum load (0.7 W), the frequency drops to 19 kHz. Thus, the proposed control provides converter operation in the entire load range with the frequency variation from 19 to 58 kHz.

To meet load regulation and transient response specifications, error amplifier EA should be designed properly. Design of the error amplifier is conducted in the frequency domain and is based on the continuous-time small-signal model which is derived in the Appendix. Stability and dynamic performance of the converter are determined by the loop gain $T_V(s) = H_{EA}(s) \cdot H_{VV}(s)$, where $H_{VV}(s) = \hat{V}_O/\hat{V}_{EA}$ is the control-to-output transfer function and $H_{EA}(s) = -\hat{V}_{EA}/\hat{V}_O$ is the EA transfer function. Equation (17) in the Appendix indicates that the control-to-output transfer function has a first-order response, and, therefore, design of the appropriate EA transfer function is relatively easy to accomplish. Note that, under the proposed control, transfer function $H_{VV}(s)$ at light loads differs from that at high loads. Namely, according to (15)–(17), both dc gain $g_{CO} \cdot r_O$ and pole frequency $f_{POLE} = 1/(2 \cdot \pi \cdot (R_C + r_O) \cdot C_F)$ of transfer function $H_{VV}(s)$ depend on the load. The frequency response of the control-to-output transfer function is plotted in Fig. 8 for load ranges A, B, and C. Fig. 8 shows that the difference between control-to-output transfer functions in ranges A and B is not significant. However, in the range C, the pole frequency decreases substantially. Therefore, the loop bandwidth is expected to be lower at very light loads than that at higher loads that is acceptable in most applications. Also, since the practical

loop bandwidth is usually in the 100 Hz – 10 kHz range, the stability margins at very light loads would not deteriorate with respect to those at higher loads. Therefore, the proposed control at light loads has no serious implications on the EA design which can be accomplished based on the small-signal characteristics at high loads, i.e., in the critical mode. Details of the small-signal modeling and design of the VF flyback converter in the critical mode are provided in [7].

IV. HARDWARE EVALUATION OF PROPOSED CONTROL

The experimental 380-V/19-V, 65-W flyback converter was implemented with the following major components: SW — MTP6N60, D — 10CTQ150, C_F — 1000 $\mu\text{F}/25$ V, controller — MC34262. Transformer parameters were: $N_P = 96$, $N_S = 19$, $L_M = 1.3$ mH.

Measured waveforms of the experimental converter with the proposed control for heavy, light, and very light loads are shown in Fig. 9. At the full load [see Fig. 9(a)], the duration of MMV output pulse V is shorter than the secondary-current fall time. At the instant when the secondary current falls to zero, the output signal B of the CCM/DCM detector in Fig. 3(a) propagates through gate G1 and after delay T_D turns on the switch. As a result, the converter operates in the critical mode. As the load decreases from 65 W to 10 W, the duration of the MMV output pulse increases from 9.5 to 11.6 μs , and it becomes longer than the fall time of the secondary current [see Fig. 9(b)]. The CCM/DCM detector output signal cannot turn-on the switch until the MMV output pulse expires. As a result, the converter operates in DCM. As can be seen from

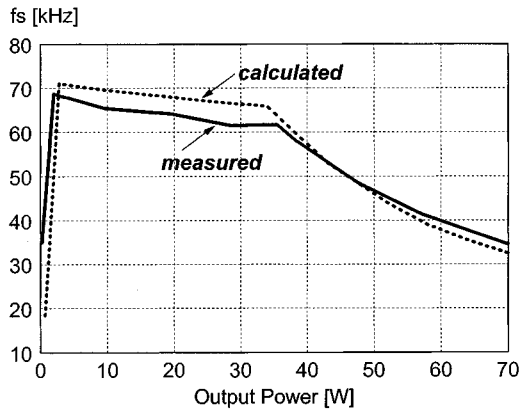


Fig. 10. Measured switching frequency of experimental prototype as a function of load.

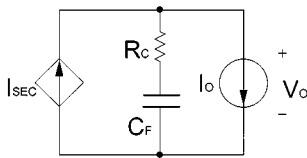


Fig. 11. Large-signal averaged model of the VF flyback converter power stage.

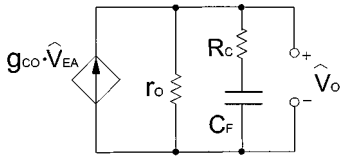


Fig. 12. Small-signal model of the VF flyback converter power stage.

Fig. 9(a) and (b), the switch turns on in the resonance valley with the minimum voltage across it at heavy and light loads. At the very light load [see Fig. 9(c)], the duration of the MMV output pulse increases to 24.3 μ s. The resonance decays significantly during the off-time, and the voltage across the switch at the turn-on instant is close to V_{IN} .

The measured switching frequency is plotted versus load in Fig. 10. For comparison, Fig. 10 also shows the calculated switching frequency curve. The converter operates in the critical mode in the 35–65 W load range. For loads below 35 W, the converter operates in DCM. When the load decreases below 2–3 W, the on-time reaches its minimum value requiring the controller to increase the off-time significantly. For this reason, the switching frequency drops down for a load below 2–3 W. This frequency drop is an additional benefit of the proposed control since it reduces the switching loss at a very light load. The shape of the frequency curves in Fig. 10 is related to the internal structure of MC34262 controller. This IC is intended for PFC applications and has an internal multiplier whose transfer characteristic is responsible for the curves' appearance.

V. SUMMARY

It was demonstrated that the constant off-time control of the VF flyback converter cannot regulate the output as the load current approaches a zero value. A simple adaptive control was proposed which regulates the output down to zero load. The proposed control also maintains the soft switching at light loads. An

additional advantage of the adaptive control is the switching frequency reduction at light loads. The proposed control was successfully implemented in the 380-V/19-V, 65-W flyback converter.

APPENDIX

The equivalent circuit, corresponding to the power stage averaged large-signal model, is shown in Fig. 11, where I_{SEC} is the average value of the transformer secondary current

$$I_{SEC} = \frac{N \cdot I_{PEAK}}{2} \cdot \frac{T_{FALL}}{T_{ON} + T_{OFF}}. \quad (13)$$

Taking (4) and (12) into account

$$I_{SEC} = \frac{V_{EA}}{2 \cdot R_S \cdot M} \cdot \frac{1}{1 + \frac{T_{OFF}}{T_{ON}}}. \quad (14)$$

The latter equation together with (1), (11), and (12) was used to derive the expression for I_{SEC} in load ranges A, B, and C

$$I_{SEC} = I_{SEC}(V_{EA}, V_O, V_{IN}) \begin{cases} \frac{V_{EA}}{2 \cdot R_S \cdot M} \cdot \frac{1}{1 + \frac{1}{(N \cdot M)}}, & \text{in range A} \\ \frac{V_{EA}}{2 \cdot R_S \cdot M} \cdot \frac{1}{1 + \tau_1 \cdot \ln\left(\frac{V_{ZD}}{V_{EA}}\right) \cdot \frac{R_S}{(L_M \cdot V_{EA})}}, & \text{in range B} \\ \frac{V_{EA}}{2 \cdot R_S \cdot M} \cdot \frac{1}{1 + \tau_1 \cdot \frac{\ln\left(\frac{V_{ZD}}{V_{EA}}\right)}{T_{ON}^{\min}}}, & \text{in range C.} \end{cases} \quad (15)$$

The small-signal model is derived by perturbing (15) around the operating point

$$\hat{I}_{SEC} = \frac{\partial I_{SEC}}{\partial V_{EA}} \cdot \hat{V}_{EA} + \frac{\partial I_{SEC}}{\partial V_O} \cdot \hat{V}_O + \frac{\partial I_{SEC}}{\partial V_{IN}} \cdot \hat{V}_{IN} \quad (16)$$

where the “hat” symbol is used to designate small-signal variables.

For the purpose of the feedback loop design, $\hat{V}_{IN} = 0$, and the small-signal model is represented by the equivalent circuit, as shown in Fig. 12, where $g_{CO} = \partial I_{SEC} / \partial V_{EA}$ and $r_O = -\partial I_{SEC} / \partial V_O$.

Based on the equivalent circuit, the control-to-output transfer function is finally derived

$$H_{VV}(s) = \frac{\hat{V}_O}{\hat{V}_{EA}} = \frac{g_{CO} \cdot r_O \cdot (1 + R_C \cdot C_F \cdot s)}{1 + (R_C + r_O) \cdot C_F \cdot s}. \quad (17)$$

REFERENCES

- [1] P. Greenland and S. Sandler, “Consumer-oriented quasi-resonant flyback converter suits broader applications,” *Power Conv. Intell. Motion Mag.*, pp. 9–19, Apr. 1988.
- [2] J. B. Lio, M. S. Lin, D. Y. Chen, and W. S. Feng, “Single-switch, soft-switching flyback converter,” *IEE Electron. Lett.*, June 1996.
- [3] “TDA 4605-3 control IC for switched-mode power supplies using MOS-transistor,” Tech. Rep., Siemens, 1997.
- [4] “Critical conduction GreenLine SMPS controller,” Tech. Rep. MC33364/D, Motorola, 1998.
- [5] “A controller family for switch mode power supplies supporting low power standby and power factor correction,” Tech. Rep. TDA-1684X, Infineon Technologies, Richmond, VA, 2000.
- [6] “L6565 Quasi-resonant controller,” Tech. Rep. AN-1326, ST, 2001.

- [7] J. Lempinen and T. Santio, "Small-signal modeling for design of robust variable-frequency flyback battery chargers for portable device applications," *IEEE Appl. Power Electron. Conf. Rec.*, vol. 1, pp. 548–554, Mar. 2001.



Yuri Panov received the Dipl.-Eng. and Ph.D. degrees in electrical engineering from the Moscow Aviation Institute, Moscow, Russia, and the M.S. degree in electrical engineering from Virginia Polytechnic Institute and State University, Blacksburg.

He is currently with Delta Products Corporation, Research Triangle Park, NC. His 17-year experience includes dc/ac, ac/dc, and dc/dc power conversion, modeling and design of large-scale power systems for aerospace applications, and design of various analog electronics circuits. His current research is focused on high-power-density offline power supplies and dc/dc converters for next generations of microprocessors.



Milan M. Jovanović (S'86–M'89–SM'89–F'01) was born in Belgrade, Yugoslavia. He received the Dipl.-Ing. degree in electrical engineering from the University of Belgrade.

Presently, he is the Vice President for Research and Development of Delta Products Corporation, Research Triangle Park, NC (the U.S. subsidiary of Delta Electronics, Inc., Taiwan, R.O.C.).